EV Charging Scheduling Under Demand Charge: A Block Model Predictive Control Approach

Lei Yang, *Student Member, IEEE*, Xinbo Geng, *Member, IEEE*, Xiaohong Guan, *Life Fellow, IEEE*, and Lang Tong, *Fellow, IEEE*

***Abstract*— This paper studies the online scheduling of electric vehicle charging by a service provider subject to a demand charge in a distribution system. Demand charge imposes a penalty on the peak power consumption over each billing period, representing a substantial cost for the service provider with a large number of clients. Because the demand charge is calculated at the end of the billing period, it poses challenges in real-time scheduling when energy demand forecasts are inaccurate, resulting in either overly conservative power consumption or substantial demand charge. We propose a block model predictive control approach that decomposes the demand charge into a sequence of stage costs. Optimality conditions on demand patterns are also presented and analyzed. Numerical simulations demonstrate the efficacy of the proposed approach.**

***Note to Practitioners*—This paper addresses a significant practical problem of minimizing the demand charge on the real-time scheduling of deferrable demands. In particular, we consider a setting where a commercial electric vehicle (EV) charging service provider has to manage the online scheduling of a large number of arriving EVs at a charging facility subject to a maximum charging power constraint and a tariff with the demand charge. A major practical challenge is to balance the tradeoff between maximizing profit in scheduling as much EV charging as possible and the need to minimize penalty on the peak charging power. We propose a model predictive control strategy that decomposes the overall demand charge into a sequence of terminal costs. Also addressed is the practical constraint arising from the mismatched EV charging decision period and the power measurement period used to compute the demand charge. Using real data collected at the Adaptive Charging Network (ACN) testbed in simulations, the proposed approach yields 8-12% improvement in operational profit over existing benchmarks, while it has yet been tested in actual charging systems. In the future research, we will address the charging scheduling under demand charge over multiple charging stations.**

***Index Terms*— Demand charge, demand side management, online scheduling, charging of electric vehicles, model predictive control (MPC).**

Manuscript received 16 December 2022; accepted 20 February 2023. Date of publication 31 March 2023; date of current version 9 April 2024. This article was recommended for publication by Associate Editor H.-J. Kim and Editor L. Moench upon evaluation of the reviewers' comments. The work of Lei Yang and Xiaohong Guan was supported by the National Key Research and Development Program of China under Grant 2016YFB0901900. The work of Xinbo Geng and Lang Tong was supported in part by the U.S. National Science Foundation under Award 1816397 and Award 1809830. *(Corresponding author: Lei Yang.)*

Lei Yang is with the Faculty of Electronic and Information Engineering, Xi'an Jiaotong University, Xi'an 710049, China, and also with the School of Electrical and Computer Engineering, Cornell University, Ithaca, NY 14850 USA (e-mail: kobela33@stu.xjtu.edu.cn).

Xinbo Geng and Lang Tong are with the School of Electrical and Computer Engineering, Cornell University, Ithaca, NY 14850 USA (e-mail: xg72@cornell.edu; lt35@cornell.edu).

Xiaohong Guan is with the Faculty of Electronic and Information Engineering, Xi'an Jiaotong University, Xi'an 710049, China (e-mail: xhguan@sei.xjtu.edu.cn).

Digital Object Identifier 10.1109/TASE.2023.3260804

I. Introduction

WE CONSIDER the problem of scheduling electric vehicle (EV) charging in an EV charging facility by a commercial service provider. The EV charging model accounts for the stochastic arrival of EVs and their charging demands, the need to constrain total charging power imposed by the distribution grid, and the costs of EV charging arising from the energy and the demand charge set by the tariff of a local utility. At a higher level, such a scheduling problem falls in the category of stochastic dynamic programming, for which the optimal solution suffers from the curse of dimensionality, making it unrealistic for practical implementations.

The importance of a carefully designed EV charging schedule is well understood, and there is extensive literature on various approaches, each capturing certain aspects of the EV charging problem; see a brief review in Section I-A. Among the most significant factors are the need to exploit the flexibility of charging demands, avoid peak-demand hours during which the energy cost is high, incorporate colocated renewables, and deal with dynamically varying electricity prices.

This paper focuses on two nontrivial but less studied aspects of centralized EV charging in a distribution system by a profit-seeking service provider: the stochastic arrival of charging demands and the high cost of the demand charge. Without a computationally tractable optimal scheduling solution, we aim to develop a suboptimal model predictive control (MPC) strategy that exploits the structure of EV charging characteristics and incorporates the demand charge as a sequence terminal cost associated with the optimization at each stage.

The centralized EV charging in a distribution system allows us to remove or deemphasize some of the complications commonly considered in the literature, some of which can be incorporated under the general MPC framework, while others become unnecessary for the problem at hand. Specifically, we assume that the marginal cost of electricity is deterministic and the demand charge price fixed as part of a long-term contract with the distribution utility. The behind-the-meter

renewable is not considered. While such resources can be incorporated in the MPC-based dynamic optimization, their significance rests primarily in the scheduling performance rather than in developing an MPC-based solution.

A. Related Work

The literature on EV charging scheduling is vast. Here we restrict our review to centralized scheduling of a large number EV chargings by a profit-seeking operator.

A significant line of contributions to the EV charging literature follows a baseline of charging optimizations involving a fixed set of EVs [1], [2], [3], [4], [5], [6], [7], [8], [9]. Most work under such formulations applies naturally to the residential EV charging problems, where distributed implementations are often important. While these approaches can be adapted to the centralized EV charging problem considered in this paper, they have very different objectives from that of a commercial EV charging service provider. Some of the missing ingredients in these models are the *stochastic* arrival/departure of charging requests, charging demands, and charging completion deadlines.

Our approach presented in this paper follows the online job-scheduling formulation where charging demands (jobs) arrive and depart sequentially with uncertainty. One line of approaches is to cast the problem as the classical (deterministic) deadline scheduling problem [10], [11], [12], [13], [14], [15] where jobs with completion deadlines are centrally scheduled in real-time. In the context of EV charging, jobs are EVs with stochastic demands, processors are EV charging connecting ports, and the operator is the scheduler. The simple and sometimes optimal deterministic scheduling schemes such as the earliest deadline first (EDF) and the least-laxity-first (LLF) algorithms remain to be the benchmarks for comparisons. These approaches treat job arrivals as deterministic and arbitrary.

The scheduling of EV charging under stochastic arrivals starts with a Markov decision process (MDP) formulation of the scheduling problem [16], [17], [18], [19], [20], [21], [22], [23], [24], [25]. The approach presented in this paper follows the problem formulation of these approaches. Recognizing that the MDP solutions are intractable in practice, efforts have been made to discover and exploit the structural properties of the problem to achieve suboptimal (sometimes asymptotically optimal) performance [21], [22], [23], [24], [25]. In particular, when the charging demand arrival is light relative to overall system charging capacity, it is shown in [23] that, without the demand charge, the Whittle's index policy [26] is asymptotically optimal. Outside the light traffic regime and without demand charge, the Less Laxity First with Later Deadline (LLF-LD) scheduling algorithm proposed in [27] exhibits near-optimal performance in simulations.

MPC, more precisely receding-horizon economic MPC (EMPC) [28], is a computationally tractable solution that often performs well in practice when dealing with optimization problems involving dynamic systems and economic objectives. Such a model fits naturally to the large-scale EV charging problem for a service provider with a profit-maximizing objective. EMPC has been applied to centralized EV charging problem in [29] and [30]. The EMPC models considered in these contributions differ considerably from our paper's approach. Halvgaard et al. [29] formulated one of the earliest EMPC approaches to EV charging that minimizes charging costs involving a fixed set of EVs over a scheduling interval. More recent work of Engel et al. [30] considers the centralized co-optimization of EV charging and building energy management systems. Missing in these formulations are the arrival and departure dynamics of EV demands and stochastic charging completion deadlines.

Demand charge can be a significant part of its cost for a profit-maximizing operator of a large EV charging service. Because demand charge is determined by the maximum power consumption (typically measured over multiple charging periods), it is nontrivial to capture such cost within each receding-horizon MPC optimization. In [8], Lee et al. proposed an MPC method that decomposed the demand charge into multiple convex problems, where heuristics were introduced to weight the demand charge to influence the performance on the overall profit. Although not designed for the EV charging problem, the work of Kumar et al. [31] and the recent paper of Risbeck and Rawlings [32] also bear significant relevance to our work. Similarly to [8], the approach of Kumar et al. [31] to incorporating the demand charge in MPC is heuristic by setting a time-varying weight at each optimization problem. Risbeck and Rawlings, on the other hand, proposed a principled approach that explicitly incorporated the demand charge as a terminal cost of each EMPC optimization in [32]. Their approach, however, is designed with respect to a reference trajectory that can only be derived from perfect demand forecasts, and the maximum consumption that sets the demand charge must be computed within a single decision interval. In practice, the EV charging decision interval can be significantly shorter than the period over which the maximum demand charge is computed, for which no existing techniques explicitly account, to our best knowledge.

B. Summary of Results and Contributions

We formulate a centralized EV charging problem as an MDP where our model captures the arrival dynamics of EVs, stochastic charging demands, and stochastic completion deadlines. A significant contribution is incorporating the demand charge in the MDP formulation and deriving a novel block economic MPC solution, referred to as BMPC, to deal with the demand charge that must be computed over multiple scheduling intervals. A key ingredient of BMPC is to transform the terminal demand charge into a sequence of stage terminal costs of each BMPC optimization by tracking the peak consumption and assessing the impact of the demand charge in each stage. Although the idea of tracking the peak demand was considered in [33], [34], and [32], BMPC differs from existing techniques in terms of the specific stage costs used in the BMPC optimization and how the peak consumption is computed over multiple scheduling intervals. To support an MPC approach for EV charging applications, we show that the

MPC solution is optimal when the traffic arrivals are clustered and sparse.

Extensive numerical simulations were performed based on the real dataset collected from the Adaptive Charging Network (ACN) testbed, which has provided an open database of EV charging since February 2016 and successfully operated and delivered over 1000 MWh to avoid tons of greenhouse gases [8]. We compared BMPC with four benchmark algorithms, including MPC with scaled demand charge (MPC-scaled), EMPC [32], MPC without demand charge (MPC-w/o) and LLF-LD [27]. Numerical results demonstrate that BMPC achieves the best performance in most cases. In particular, BMPC can achieve 8% more total reward than the second-best approach when EV charging requests are stochastic. Compared with MPC-w/o and LLF-LD, BMPC can obtain more than 12% total reward on average, even under 80% forecast accuracy.

The remainder of this paper is organized as follows. We formulate the EV-DC problem as an MDP in Section II. In Section III, we develop BMPC as the online scheduling algorithm and demonstrate the numerical results in Section IV. Finally, we conclude the paper in Section V.

II. EV Charging Under Demand Charge

We consider the problem of scheduling of EV charging under demand charge (EV-DC) at a public facility [16], [18], [23], [35], [36], where EVs with charging demands arrive stochastically, each with a random amount of energy request and specified deadline for completion [23].

A. Nominal Model Assumptions

Consider an EV charging facility with N chargers (charging ports) as illustrated in Fig. 1. EVs arriving at the charging facility are assigned randomly to one of the available chargers. We assume that, upon arrival, the EV reveals to the operator its charging demand and deadline for completion.[1]

The operator faces a deadline scheduling problem, aimed at completing as many EV charging jobs as possible by their deadlines. The reward for the operator is the revenue from serving EV demands. The cost, on the other hand, comes from the electricity consumed in EV charging, the demand charge imposed by the distribution utility, and the penalty when the charging demands are not fulfilled. The operator also faces the constraint that only a finite number of chargers can be activated simultaneously due to transformer constraints from the distribution circuit.

We consider a finite scheduling horizon $\mathcal{T}$, indexed by $t \in \mathcal{T} := \{0, 1, \cdots, T-1\}$. Some of the key details and assumptions of EV-DC are outlined below.

[1]For EV charging at public parking facilities at shopping and office complex, a customer may not stand by until the charging is completed. It is therefore natural that a deadline for completion is included in the charging demand so that the customer can be away and return at the time of completion [37], [38].

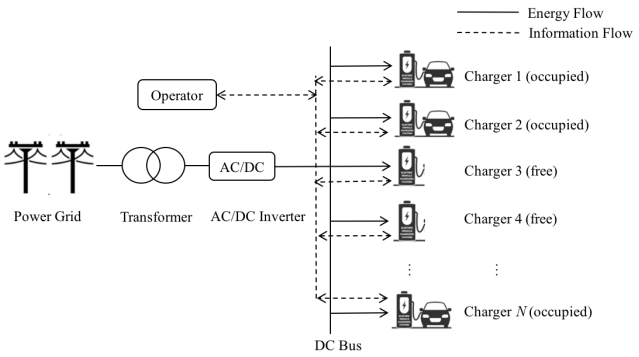

Fig. 1. Schematic of EV-DC at a public facility.

A1) At each interval,[2] a charger can only work on one EV, and each EV can receive service from only one charger at any given time.

A2) Each charger has a constant charging rate R at each interval $t \in \mathcal{T}$. The charging decision at interval t for the i-th charger is a binary variable $u_{i,t}, i = 1, \ldots, N$, with 1 activating and 0 deactivating the charging port.

A3) The EV arriving at the i-th charger at the beginning of interval t_0 reveals random D_{i,t_0} (total amount of energy to be completed) and T_{i,t_0} (deadline). An EV will be automatically removed at the end of deadline.

A4) The operator receives a per unit reward π^r and pays a time-varying charging cost π^e_t if it serves an EV at interval t. For simplicity, we assume that parameters π^r and $\{\pi^e_t\}_{t=0}^{T-1}$ are deterministic. The proposed approaches can be easily extended towards stochastic settings.

A5) If the total charging demand of EV i is not completed before it leaves, then a penalty occurs at unit price q. We also assume that the penalty price is greater than the largest charging cost over the whole horizon, *i.e.*, $q \geq \pi^e_t, \ \forall t \in \mathcal{T}$.

Remark 1: Comments and justifications for these assumptions are in order. Assumption A1 is standard and holds for most existing charging stations [39]. The on-off charging model assumed in A2 is a reasonable approximation to the actual charging profile[3] [40], and it can be extended to cases with continuously varying charging rates [8]. A3 assumes that random charging requests and completion time are known upon arrival, which is necessary for quality-differentiated EV charging services. Some commercial and business EV charging facilities impose the duration of charging [37], [38]. A4 is the standard assumption that the price of charging (per kWh) is the same for all the EVs [41]. The marginal cost of EV charging (mostly from the energy cost for the service provider) is constant for EVs processed within the same interval t. Generalizations to the time-varying case such as [42] are possible. Because there are physical constraints (*e.g.*, from

[2]Throughout the paper, we use "stage" to index optimization and "interval" to index time (decision epoch).

[3]In practice, the charging rate may vary depending on the SoC, especially when the battery is nearly fully charged.

power system transformers) that limits the amount of power delivery at any given time, the EV charging service provider may not be able to complete charging requests by the deadline when the demand is high. In such cases, we assume in A5 that the service provider must compensate the customer with the penalty price q to enhance the quality of charging services [43], [44], where the soft deadline can be hardened by setting the non-completion penalty much higher than the charging cost. Thus it is always optimal (*i.e.*, reward maximizing) to finish as many EV requests as possible.

B. Problem Formulation

EV loads are flexible demands such that their services can be delayed. By shifting part or all of the demands, EV-DC has strong inter-temporal dependencies. We present in section a Markov decision process (MDP) model for EV-DC [21], [27], subject to various constraints including the maximum charging rate, time-varying electricity price and a monthly demand charge.

1) Exogenous Stochastic Input $\boldsymbol{\xi}$: The input of EV-DC model is a vector random process that models the arrivals of EV demands at individual chargers. The occupancy of each charger is an on-off process with the charger being occupied for the duration of the EV charging deadline and being idle for the duration of a Bernoulli process based on with parameter α_i set by the overall arrival rate of the EV demands.[4] At the beginning of an occupied period of charger i, say at t_0, an EV arrives with random energy demand D_{i,t_0} and random deadline T_{i,t_0}. Thus the input process at charger i is given by $\xi_{i,t} = (D_{i,t_0}, T_{i,t_0})$ for $t = t_0, \ldots, T_{i,t_0}$. When the charger is idle, $\xi_{i,t} = (0, 0)$. With probability α_i, $\xi_{i,t} = (0, 0)$ transitions to $\xi_{i,t+1} = (D_{i,t+1}, T_{i,t+1})$.

2) System State and State Evolution: The state of charger i at interval t is given by a tuple $x_{i,t} = (r_{i,t}, \tau_{i,t})$, where $r_{i,t}$ represents the remaining demand to be served by deadline $T_{i,t}$ at charger i and $\tau_{i,t} = T_{i,t} - t$ the lead time to the EV's deadline at interval t. Hence, the system state is modeled as

$$x_{i,t+1} = \begin{cases} x_{i,t} - (u_{i,t}, 1) & \text{if } \tau_{i,t}) > 1, \\ \xi_{i,t} & \text{if } \tau_{i,t} \leq 1. \end{cases} \tag{1}$$

Note that when the charger is free, its state is $(0, 0)$. When there is no EV arriving at charger i, the state of the charger remains at $(0, 0)$.

3) Constraints: The total amount of power used for charging at one interval is limited by

$$\sum_{i=1}^{N} u_{i,t} \leq M, \ t \in \mathcal{T}, \tag{2}$$

where M denotes the maximum number of simultaneous chargers allowed by the maximum power constraint of the local transformer ($M < N$). The charger cannot be activated when no EV is connected:

$$u_{i,t} \leq x_{i,t}, \ i \in \{1, \ldots, N\}, \ t \in \mathcal{T}. \tag{3}$$

[4]The assumption on the Bernoulli process is made for the theoretical analysis shown in Section III-C, whereas the algorithm proposed in this paper does not require specific EV arrival process. Thus ACN dataset can be used for the numerical tests shown in Section IV.

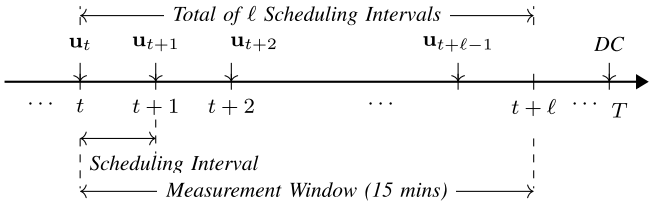

Fig. 2. Temporal structure of ℓ scheduling intervals and one measurement window under the monthly demand charge (DC). The average power consumption over a measurement window is calculated as $\frac{R}{\ell}(\mathbf{u}_t + \cdots, \mathbf{u}_{t+\ell-1})$.

4) Demand Charge: Based on the pricing of the demand charge, the average power consumption over ℓ consecutive scheduling intervals is calculated for each non-overlapping measurement window.[5] The *maximum* value among these measurement windows for the demand charge is represented by variable ψ and calculated as follows:

$$\psi = \max_{t \in \mathcal{T}'} \frac{R}{\ell} \sum_{\tau=t}^{t+\ell-1} \sum_{i=1}^{N} u_{i,\tau}, \tag{4}$$

where $\mathcal{T}' = \{0, \ell, 2\ell, \ldots, T - \ell\}$ denotes the set of the beginning interval of each measurement window. Thus the demand charge is computed as $\mathcal{C}(\psi) = \pi^d \psi$, where π^d is the unit price of the demand charge.

Remark 2: For the computation of the demand charge, practically the length of a measurement window may not match the control resolutions, *e.g.*, operating a charger at every 1-5 minutes for fast charging rather than 15 minutes [45]. Therefore, we introduces an integral parameter ℓ representing the total number of scheduling intervals contained in a measurement window, *i.e.*, the length of a measurement window is identical to ℓ intervals, and its value obviously relies on the specific application settings, as shown in Fig. 2.

5) Reward: The reward collected from all the EVs at interval t is given by

$$\mathcal{G}(\mathbf{x}_t, \mathbf{u}_t, \boldsymbol{\xi}_t) = R\Delta \left[(\pi^r - \pi_t^e) \sum_{i=1}^{N} u_{i,t} - q \sum_{i \in \mathcal{J}_t} (r_{i,t} - u_{i,t}) \right] \tag{5}$$

where Δ denotes the length of a scheduling interval and $\mathcal{J}_t$ the set of EVs that will leave at interval $t + 1$, *i.e.*, $\mathcal{J}_t := \{i : \tau_{i,t} = 1\}$.

6) MDP Formulation: The objective of EV scheduling is to find the optimal control policy $\{\mu_t^*\}_{t \in \mathcal{T}}$ to maximize the expected total reward in the presence of the demand charge. At each interval t, a control law maps states to controls:

$$\mathbf{u}_t = \mu_t(\mathbf{x}_t, \boldsymbol{\xi}_t). \tag{6}$$

[5]For demand side management applications of power systems, the length of a measurement window is often 15 or 30 minutes. In this paper we fix the value at 15 minutes.

Given an initial state $\mathbf{x}_0$, the EV-DC can be formulated as an integer linear program:

$$\max_{\{\mu_t\}_{t\in\mathcal{T}}} \ \mathbb{E}_{\boldsymbol{\xi}}\left[\sum_{t=0}^{T-1}\mathcal{G}(\mathbf{x}_t,\mathbf{u}_t,\boldsymbol{\xi}_t)-\mathcal{C}(\psi)\right] \quad \text{s.t. } (1)(2)(3)(4)(6), \tag{7}$$

Remark 3: The model defined in (7) can be easily extended to a much broader class of deferrable load scheduling under demand charge problems beyond EV-DC, such as applications mentioned in [46] and [33]. The main difficulties of dealing with the demand charge in the MDP framework come from the *mismatch of different timescales*. In particular, three timescales coexist in the formulated model (See Fig. 2):

(1) the control $\mathbf{u}_t = \mu_t(\mathbf{x}_t, \boldsymbol{\xi}_t)$ happens at every $t \in \mathcal{T} = \{0, 1, \cdots, T-1\}$;
(2) the peak average consumption that sets the demand charge is calculated at the end of each measurement window at $t = \{\ell, 2\ell, \cdots, T\}$;
(3) the demand charge is imposed at the terminal T.

Because the reward $\mathcal{G}(\cdot)$ is realized at every interval t whereas the demand charge $\mathcal{C}(\psi)$ is levied at the end of the entire control horizon, it is challenging to balance the trade-off between the immediate reward and the uncertain demand charge set at the end of the scheduling horizon.

III. Block Model Predictive Control

We present a variation of the standard MPC scheduling to address two demand charge related issues. The first arises from the mismatch between the EV charging control intervals and the demand charge measurement periods. Instead of realizing a single decision in each decision epoch in the traditional MPC, BMPC realizes a block of decisions. The second arises from the need of appropriating the terminal demand charge cost to each stage decision. The proposed framework is termed *Block* MPC because the rolling window moves a *block* of ℓ intervals at a time.

A. Block Model Predictive Control Under Demand Charge

To address the timescale mismatch issues arising from the demand charge (see *Remark 2*), we introduce an additional system state ϕ_t at every interval t, which represents the highest average consumption over an ℓ-sized measurement window *until* interval t. The new state variable ϕ_t evolves according to

$$\phi_{t+1} = \begin{cases} \max\left\{\phi_t, \dfrac{\sum_{\tau=t-\ell+1}^{t}\sum_{i=1}^{N} u_{i,\tau}}{\ell}\right\} & \text{if } t+1 \in \mathcal{T}' \\ \phi_t & \text{otherwise,} \end{cases} \tag{8}$$

Note that $\phi_{t+1} \geq \phi_t$ for every $t \in \mathcal{T}$. Therefore, given the system state $\mathbf{x}_0$ and ϕ_0, the EV-DC (7) can be equivalently formulated as:

$$\max_{\{\mu_t\}_{t\in\mathcal{T}}} \ \mathbb{E}_{\boldsymbol{\xi}}\left[\sum_{t\in\mathcal{T}}\mathcal{G}(\mathbf{x}_t,\mathbf{u}_t,\boldsymbol{\xi}_t)-\mathcal{C}(\phi_T)\right] \quad \text{s.t. } (1)(2)(3)(6)(8), \tag{9}$$

With the amended state, it is much easier to apply the idea of MPC-based approaches on the reformulated problem (9). Generally, MPC considers the optimization problem of a shorter horizon $\{t, \cdots, t+W\}$ and utilizes a predicted trajectory $\{\hat{\boldsymbol{\xi}}_k\}_{k=t}^{t+W-1}$. As a result, BMPC solves the following deterministic problem for a forecast window of length W with the current state $\mathbf{x}_t$ and ϕ_t at $t \in \mathcal{T}'$:

$$\max_{\{\mathbf{u}_k\}_{k=t}^{t+W-1}} \ \sum_{k=t}^{t+W-1}\mathcal{G}\left(\mathbf{x}_k,\mathbf{u}_k,\hat{\boldsymbol{\xi}}_k\right)-\mathcal{H}(\phi_{t+W}) \tag{10a}$$

$$\text{s.t. } x_{i,k+1} = \begin{cases} x_{i,k}-(u_{i,k},1) \text{ if } \tau_{i,k}>1, \\ \hat{\xi}_{i,k} \text{ if } \tau_{i,k}\leq 1, \end{cases} \tag{10b}$$

$$\sum_{i=1}^{N} u_{i,k} \leq M, \tag{10c}$$

$$u_{i,k} \leq x_{i,k}, \ i \in \{1,\ldots,N\} \tag{10d}$$

$$\phi_k \text{ updates as in (8)}, \quad k = t,\ldots,t+W-1, \tag{10e}$$

where $\mathcal{H}(\phi_{t+W})$ is the BMPC end-of-horizon cost (to be specified in Section III-B). The main difference between BMPC and the nominal MPC is the *block* structure. Instead of moving from t to $t+1$, BMPC moves one block (ℓ intervals) at each stage, *i.e.*, from t to $t+\ell$. The optimal controls of (10) in the first block $\{\mathbf{u}_t^*, \cdots, \mathbf{u}_{t+\ell-1}^*\}$ will be implemented. Others $\{\mathbf{u}_{t+\ell}^*, \cdots, \mathbf{u}_{t+W-1}^*\}$ are only advisory.

Remark 4: Different from those EMPC methods [28] that aim to minimize the gap between a controlled system and a reference in process control engineering, BMPC aims to maximize total reward for EV charging applications where stability and tracking error are not of concern.

Remark 5: Generally, the complexity of BMPC grows exponentially with the number of unfinished jobs, since the decision variables are integers. However, the state-of-art commercial solvers such as Gurobi and CPLEX work efficiently to handle integer programs with over thousands of variables [47], [48], and the computation time of the proposed approach is in an acceptable range, as shown in Section IV.

The BMPC approach is summarized as Algorithm 1. Two factors affect the performance of BMPC: an end-of-horizon cost $\mathcal{H}(\phi_{t+W})$, and an initial guess on the maximum average consumption ϕ_0. The choice of the end-of-horizon cost $\mathcal{H}(\phi_{t+W})$ lies at the heart of BMPC solution to EV-DC. Detailed discussions and comparisons are in Section III-B. The initial guess ϕ_0 can be derived by the mainstream techniques for load forecasting at the distribution level [49], [50], such as regression or neural networks by using the historical demands as the training samples. The influence on this value is also discussed in Section III-C.

Algorithm 1 BMPC Under Demand Charge

Initialization: Initialize system with $\mathbf{x}_0$, ϕ_0, W.
for $t \in \{0, \ell, \cdots, T-\ell\}$ **do**
  Observe the system current state $\mathbf{x}_t$, the up-to-date highest average consumption ϕ_t and the EV arrival $\boldsymbol{\xi}_t$;
  Forecast the future EV arrivals $\{\hat{\boldsymbol{\xi}}_k\}_{k=t+1}^{t+W-1}$ over $t+1$ to $t+W-1$;
  Solve the BMPC Problem (10);

$$\{\mathbf{u}_k^*\}_{k=t}^{k+W-1} = \text{BMPC}(\mathbf{x}_t, \phi_t, \{\hat{\boldsymbol{\xi}}_k\}_{k=t}^{t+W-1}) \tag{11}$$

  Take the first block (ℓ intervals) of controls from the solution to (10): $\mathbf{U}_t^* = (\mathbf{u}_t^*, \ldots, \mathbf{u}_{t+\ell-1}^*)$
  for $j \in \{t, t+1, \ldots, t+\ell-1\}$ **do**
    Observe the system state $\mathbf{x}_j$ and the input $\boldsymbol{\xi}_j$;
    Take $\mathbf{u}_j^* = \mu_j^*(\mathbf{x}_j, \boldsymbol{\xi}_j)$ as the decision at j and update the system state to $\mathbf{x}_{j+1}$ according to (1);
    Update ϕ_j according to (8).
  end for
end for

B. BMPC End-of-Horizon Cost $\mathcal{H}(\phi_{t+W})$

Intuitively, good choices of the end-of-horizon cost $\mathcal{H}(\phi_{t+W})$ should reflect the amortization of the demand charge in the current interval t. Some primitive forms could be:

$$\mathcal{H}(\phi_{t+W}) := \mathcal{C}(\phi_{t+W}), \quad t \in \mathcal{T}', \tag{12a}$$

$$\mathcal{H}(\phi_{t+W}) := \frac{W}{T}\mathcal{C}(\phi_{t+W}), \quad t \in \mathcal{T}'. \tag{12b}$$

However, these two choices perform poorly in practice because (12a) imposes the demand charge *over the entire control horizon* T on the rolling window. When $W \ll T$, the demand charge $\mathcal{C}(\phi_{t+W})$ would dominate the total reward of the rolling window. As a result, the solution in this setting will often be so conservative that the operator would rather sacrifice most of the reward than incur a large demand charge cost. In addition, (12a) fails to capture the fact that demand charge is only posed for the peak consumption.

A slightly better choice is (12b), which splits the demand charge *equally* among T intervals. This choice essentially assumes that the states of EV charging loads within each measurement window are almost identical, which is often not true in practice.

We propose a more judicious choice

$$\mathcal{H}(\phi_{t+W}) := \mathcal{C}(\phi_{t+W} - \phi_t), \ t \in \mathcal{T}'. \tag{13}$$

The rationale behind (13) is twofold. First, it is clear that $\phi_{t+W} \geq \phi_t$ always holds true according to (8). If the peak consumption of the current rolling window $\{t, \cdots, t+W\}$ is no higher than the previous one ($\phi_{t+W} = \phi_t$), no additional cost should be considered, *i.e.*, $\mathcal{H}(\phi_{t+W}) = 0$. Additional cost occurs only when the peak consumption increases, *i.e.*, $\phi_{t+W} > \phi_t$.

Remark 6: For EV-DC where the demand charge cost function is linear, the BMPC end-of-horizon cost can be further justified. In this case, we have

$$\mathcal{C}(\phi_T) = \mathcal{C}(\phi_0) + \sum_{t\in\mathcal{T}'} \mathcal{H}(\phi_{t+W}) = \mathcal{C}(\phi_0) + \sum_{t\in\mathcal{T}} \mathcal{C}(\phi_{t+1} - \phi_t), \tag{14}$$

which enables us to define a revised reward function that considers the cost of demand charge at each $t \in \mathcal{T}$:

$$\mathcal{V}(\mathbf{x}_t, \mathbf{u}_t, \boldsymbol{\xi}_t, \phi_t) := \mathcal{G}(\mathbf{x}_t, \mathbf{u}_t, \boldsymbol{\xi}_t) - \mathcal{C}(\phi_{t+1} - \phi_t). \tag{15}$$

It is clear that (13) is a direct result of formulating BMPC using (15). The equation above reveals that (13) embeds the demand charge cost, which occurs at the end of control horizon, into each stage as decomposed in (15). Therefore, (13) effectively avoids the inferior performance by directly using the demand charge structure such as (12a) or (12b).

C. Optimality of BMPC

MPC rarely achieves optimality in general. To justify and support the proposed solution, we consider the particular case when the proposed BMPC happens to be optimal. Specifically, we assume that EV arrivals are clustered during operation hours; many EVs sometimes arrive close to one another, and no EV arrives between clusters.[6] Such characteristics are supported by the real-data set collected at the ACN testbed.

To formalize the "clustered arrival characteristics", we introduce the notion of the decoupling interval.

Definition 1: An interval $t^d \in \mathcal{T}$ is a decoupling interval if $(x_{i,t^d}, \xi_{i,t^d}) = (0, 0)$ for all $i \in \{1, \ldots, N\}$.

For the EV-DC problem, a decoupling interval corresponds to the time period when the total charging demands are zero, *i.e.*, energy demands of all the parking EVs have been finished before t^d and no new ones arrive at t^d. We also have several assumptions:

A7) The length of a scheduling interval of (7) is the same as the measurement window, *i.e.*, $\ell = 1$.
A8) For $\forall t \in \mathcal{T}$, the forecasts of the exogenous variables $\{\boldsymbol{\xi}_k\}_{k=t+1}^{t+W-1}$ are accurate within the forecast window.

For a given arrival trajectory $\boldsymbol{\xi}$ with an initial state $\mathbf{x}_0$, let $J_{\boldsymbol{\xi}}^{\text{BMPC}}(\mathbf{x}_0, \phi_0)$ be the total reward produced by Algorithm 1, $J_{\boldsymbol{\xi}}^*(\mathbf{x}_0)$ the optimal reward of (7) and $\psi_{\boldsymbol{\xi}}^*$ the corresponding optimal maximum average consumption. Then we present the following optimality conditions of BMPC:

Proposition 1: Under Assumption A7 and A8, for every arrival trajectory $\boldsymbol{\xi}$ and initial condition $\mathbf{x}_0$, BMPC achieves optimal reward, *i.e.*, $J_{\boldsymbol{\xi}}^{\text{BMPC}}(\mathbf{x}_0, \phi_0) = J_{\boldsymbol{\xi}}^*(\mathbf{x}_0)$, if

(i) each stage optimization includes at least one decoupling interval,
(ii) the initial estimate of the maximum consumption is perfect, *i.e.*, $\phi_0 = \psi_{\boldsymbol{\xi}}^*$.

The proof of Proposition 1 is given in Appendix A.

Remark 7: We take Proposition 1 not as a theoretical guarantee in practice but as a theoretical ideal for EV charging in practice as the two conditions for optimality are strong; a justification of these conditions is in order.

[6]Theoretically, under the general Markovian arrival model, there are always periods when no job arrives.

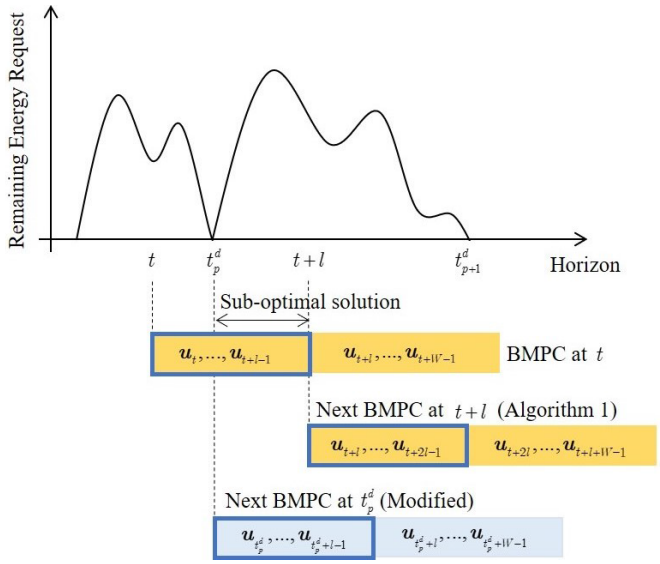

Fig. 3. Demonstration of optimality of BMPC under $\ell > 1$.

The first condition on traffic pattern implies that the arrival traffic is bursty and clustered, which has been observed in practice [51] and justified by the ACN dataset (see Section IV-C). The specific condition in (i), however, depends on the window size used in BMPC. In practice, the window size is chosen a priori, which may not guarantee (i). In such cases, one can create virtual decoupling intervals by eliminating some jobs from scheduling and paying for the penalty for those unscheduled jobs. The optimal selection of jobs for elimination requires further study and is outside the scope of this paper.

The second condition on the perfect initial estimation of $\psi_{\boldsymbol{\xi}}^*$ cannot generally hold. In practice, $\psi_{\boldsymbol{\xi}}^*$ is estimated using historical data and is bound to have errors. Empirically, we find in our experiments that the performance of BMPC is not sensitive to the estimation error, and the loss of total reward diminishes when the total scheduling horizon is long. In our simulations, the performance loss could be negligible when the estimation errors are below 10% (see Section IV-D).

Remark 8: Proposition 1 enables us to operate BMPC by less number of stage optimizations for EV-DC problems. Suppose there are total of P ($P \geq 1$) decoupling intervals in an arrival trajectory $\boldsymbol{\xi}$, indexed by t_p^d, $p = 1, \ldots, P$. The first condition indicates that the schedules before and after any t_p^d are only coupled by $\phi_{t_p^d}$. The second condition gives the optimal threshold on the maximum average consumption for all the BMPC problems, *i.e.*, $\phi_{t_p^d} = \psi_{\boldsymbol{\xi}}^*, \forall p$. Therefore, when BMPC starts at the beginning of each t_p^d, it always produces the optimal solution over t_p^d to $t_{p+1}^d - 1$, thus the next BMPC problem can start directly at t_{p+1}^d but not necessarily $t+1$.

Remark 9: To guarantee the optimality of BMPC when the system has the setting $\ell > 1$, A7 can be further relaxed by slightly modifying Algorithm 1, as demonstrated in Fig. 3. Suppose BMPC is running at t from an optimal state $\mathbf{x}_t^*$ and we take the decisions of the first block (the blue frame). Clearly, $\{\mathbf{u}_t, \ldots, \mathbf{u}_{t_p^d-1}\}$ produced by BMPC are the optimal schedules for the demands between t and t_p^d, whereas the rest $\{\mathbf{u}_{t_p^d}, \ldots, \mathbf{u}_{t+\ell-1}\}$ are sub-optimal since only part of the demand information has been considered. If the next BMPC starts at $t+\ell$, the decisions of the corresponding block are still sub-optimal, hence BMPC would never reach the optimum under $\ell > 1$. To mitigate this effect, we only need to take decisions $\{\mathbf{u}_t, \ldots, \mathbf{u}_{t_p^d-1}\}$ and start the next BMPC at t_p^d. Thus, with the optimality conditions in Proposition 1 satisfied, BMPC also produces an optimal solution under $\ell > 1$.

TABLE I
PARAMETER SETTINGS

Parameter	Value	Note
N	50	Total Number of Chargers
R	7.04 kW	Constant Charging Power (Level-2 Charger)
M	25	Maximum Number of Simultaneous Chargers
π_r	0.2 \$/kWh	Charging Reward
q	0.3 \$/kWh	Penalty Price

IV. NUMERICAL RESULTS

To evaluate the online algorithm proposed in Section III, we used a large-scale EV charging dataset, collected from a smart charging facility at Caltech on the ACN testbed.[7] The relevant parameters were summarized in Table I. We assumed that the time-varying electricity prices were deterministic and collected from the Electric Reliability Council of Texas (ERCOT).[8] Note that we set $\pi_r > \max_{t \in \mathcal{T}} \pi_t^e$ and $q > \pi_r$ to encourage chargers to serve as many charging requests as possible rather than cause large penalty. All the simulations were conducted by a computer with i7-10700 CPU and 16 GB RAM using MATLAB and Gurobi.

A. Aggregated EV Loads

To investigate the impact of the demand charge under different volumes of traffic, we generated a series of charging loads based on the original dataset, by aggregating the EVs arriving during the same time period on each day into one day. For example, 2-day aggregation level represents the one-day EV loads that are aggregated from a two-day ACN dataset, as shown in Table II. To quantify the traffic of these aggregated data, we adopted the following metric:

$$\text{Intensity} = \frac{\sum_{t_0 \in \mathcal{T}_a} \sum_{i \in \{1,\ldots,N\}} D_{i,t_0}}{RMT} \times 100\%, \qquad (16)$$

where $\mathcal{T}_a$ denotes the horizon of the aggregation level a. We increased the average intensity (over 30 trajectories) of the original traffic from 5% to 29%. In the subsequent sections, all the simulations were conducted based on these aggregated one-day data with different intensities. Furthermore, to balance the weight of the demand charge, we scaled down the monthly demand charge price[9] to a single day and varied it from 0.2

[7]The details of this facility can be found in [52] and the data is available at http://ev.caltech.edu

[8]We adopted Day-ahead Market (DAM) prices. Available at http://www.ercot.com/mktinfo/dam

[9]For simplity, we assume fixed monthly demand charge price that ranges from 6 \$/kW to 18 \$/kW [34].

TABLE II
AGGREGATION OF EV LOADS

Aggregation Level (a)	Original	2-Day	3-Day	4-Day	5-Day
Average Intensity	5%	11%	17%	24%	29%

\$/kW to 0.6 \$/kW, where the length of a measurement window was still fixed at 15 minutes.

B. On Gap to Optimality

For the optimal offline charging solution, an integer program that defined the *deterministic* EV-DC was solved to compute the upper bound of the total reward by using realizations of the EV loads from each arrival trajectory $\boldsymbol{\xi}$, as shown below:

$$J^*(\boldsymbol{\xi}) = \max_{\{\mathbf{u}_t\}_{t\in\mathcal{T}}} \sum_{t=0}^{T-1} \mathcal{G}(\mathbf{x}_t, \mathbf{u}_t, \boldsymbol{\xi}_t) - \mathcal{C}(\psi_{\boldsymbol{\xi}})$$
$$\text{s.t. } (1)(2)(3)(4). \tag{17}$$

By solving (17), we also obtained the optimal demand charge. Furthermore, three related MPC approaches and one index rule were included as benchmarks in our comparison studies: MPC with scaled demand charge (MPC-scaled), EMPC [32], MPC without demand charge (MPC-w/o) and LLF-LD [27] (see Appendix B). Then we ran each algorithm and computed its total reward gap to the upper bound (in percentage) as the performance measure. For a given scenario, we simulated all the methods over 30 trajectories and reported the average performance.

C. Performance Under Perfect Forecast

This section validates the performance of BMPC and other benchmarks under the ideal scenario, where we assume all the clients use reservation apps to offer accurate information on EV arrivals, charging demands and deadlines.

1) Single-Resolution Case ($\ell = 1$): We first considered the case when the resolution of measurement window matched that of the decision, *i.e.* $\ell = 1$ ($\Delta = 15$ minutes). In this case, BMPC operated at the same timescales as the other MPC-based benchmarks and the forecast window length was set to $W = 4$ hours.

Fig. 4a showed the performance of BMPC with other methods under different intensities of EV loads (x-axis) at a fixed demand charge price 0.3 \$/kW, where the average gaps to the upper bound over all the sampled trajectories (y-axis) were compared. The best method was EMPC [32], which actually reached the upper bound (0% gaps at all traffic levels) because it tracked the optimal reference trajectory. BMPC also produced the optimal solutions before the intensity of the EV loads reached 17%, where all the optimality conditions of BMPC could be met and therefore validated Proposition 1. Then slightly bigger gaps were shown when the EV loads went more intensive, since the number of the decoupling intervals became less and the optimality conditions could not be held at 17%-intensity and the above. Consequently, a 0.6% gap rose up at 29%-intensity. The other methods (MPC-scaled, MPC-w/o and LLF-LD) had much larger gaps (near 40% at most) and showed better performance when the aggregation level increased. This was due to the less flexibility of scheduling so that the demand charge tended to be close to each other.

Another factor that affects the performance of BMPC is the parameter M that limits the number of simultaneously activated charging. According to (16), decreasing the value of M is equivalent to increasing the traffic intensity. In Fig. 4b, we showed that the variation of M had the minimal influence on the gap to optimality of BMPC.

Then we fixed the traffic intensity at 17% and demonstrated the average performance gaps of BMPC and other methods with the variation of the demand charge prices, as shown in Fig. 4b. EMPC [32] obtained the optimal reward over all the demand charge prices, while the results of BMPC were also close, showing only 1% gap when the demand charge price reached 0.6 \$/kW. The gap produced by MPC-scaled had a steady growth from 0 to 35% since its fixed weight of the demand charge could not accommodate high demand charge prices. For the methods that do not consider demand charge, MPC-w/o and LLF-LD both experienced rapid increase as the demand charge price was over 0.4 \$/kW, hitting over 100% due to the large demand charge costs.

2) Multi-Resolution Case ($\ell = 3$): In practice, the resolution of control can be significantly finer than that of the demand charge measurement. For example, the measurement window size can be 15 minutes whereas the EV charging decisions can be made at the one to five minute resolution, *i.e.*, ℓ = 3-15. The results presented in this section are from simulations with $\ell = 3$, *i.e.*, $\Delta = 5$ minutes.

Fig. 5a illustrated the performance of BMPC with the benchmarks over varied intensity of EV loads at a fixed demand charge price 0.3 \$/kW. Although Proposition 1 did not hold when $\ell = 3$, the average gap produced by BMPC was close to the optimal at light traffic regime and less than 1% even the traffic level reached 29%-intensity. On the other hand, EMPC [32] showed sub-optimal solutions (between 2% and 10%) compared to the $\ell = 1$ case, which resulted from the mismatching of the timescales of peak consumption from the reference trajectory (see (31) and (32) in Appendix B). The performance of the rest of the methods, MPC-scaled, MPC-w/o and LLF-LD, all had improvements when the EV loads became heavier. Due to the consideration of the demand charge, MPC-scaled outperformed MPC-w/o and LLF-LD by 4% and 2% on average, respectively.

The influence of the demand charge prices was also compared in Fig. 5b, where the traffic intensity was also fixed at 17% as the previous section. BMPC was the best method to handle the increase of the demand charge price, making only 1.5% gap at 0.6 \$/kW. The performance of EMPC gradually deviated from the optimum compared to the $\ell = 1$ case and peaked at 6%. MPC-scaled had less than 2% performance gap when the demand charge price was below 0.2 \$/kW, whereas it caused larger gaps (over 10%) as the demand charge was more expensive. As for MPC-w/o and LLF-LD, they both showed a fast degradation on the total reward (at around 30%), resulting from the ignorance of the increasing demand charge costs.

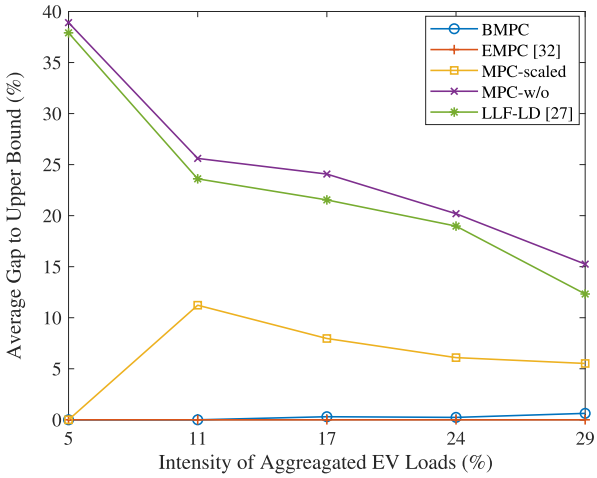

(a) Performance comparisons under different intensity levels at scaled demand charge price 0.3 $/kW

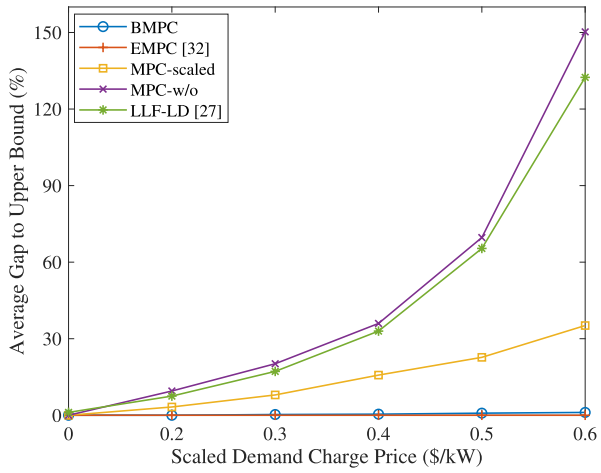

(b) Performance comparisons at different demand charge prices under 17% intensity level

Fig. 4. Average performance gap to the upper bound under perfect forecast with the system setting $\ell = 1$. The average computation time of the BMPC problems is 0.66s.

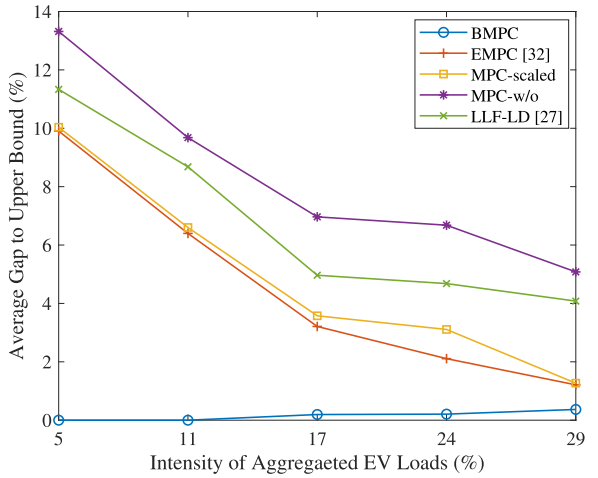

(a) Performance comparisons under different intensity levels at scaled demand charge price 0.3 $/kW

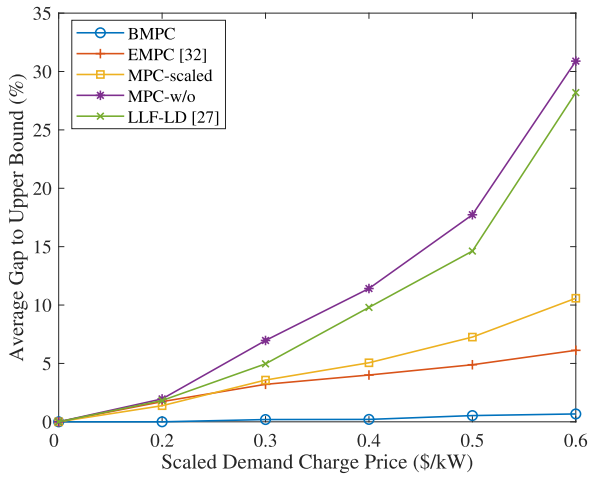

(b) Performance comparisons at different demand charge prices under 17% intensity level

Fig. 5. Average performance gap to the upper bound under perfect forecast with the system setting $\ell = 3$. The average computation time of the BMPC problems is 0.86s.

D. Performance Under Forecast Errors

This section investigates the performance of BMPC and the benchmarks under forecast errors. Here we mainly focuses on the multi-resolution case ($\Delta = 5$ minutes), which fits the practical settings but has been less addressed by the existing works.

Although the reservation mechanism can be adopted, some clients may not follow their reservations. For an EV i that actually arrives at t_0 with D_{i,t_0}, we assume a probability δ_r $(0 < \delta_r < 1)$ that the reservation information on this EV is not accurate. If so, its arrival time and the energy demand reported on the reservation apps were uniformly sampled from $[t_0(1-\delta_a), t_0(1+\delta_a)]$ $(0 < \delta_a < 1)$ and $[D_{i,t_0}(1-\delta_e), D_{i,t_0}(1+\delta_e)]$ $(0 < \delta_e < 1)$, respectively. Meanwhile, the forecast on the initial value ϕ_0 for BMPC was set as $(1-\delta_m)\psi^*_{\boldsymbol{\xi}}$ $(0 < \delta_m < 1)$. As shown in Table III, we set up four cases to demonstrate the influence of the forecast errors under different demand intensities and demand charge prices.

TABLE III
CASES FOR SIMULATIONS UNDER FORECAST ERRORS

Sequence	Setting
Case I	17%-intensity, scaled $\pi^d = 0.3$ $/kW
Case II	17%-intensity, scaled $\pi^d = 0.5$ $/kW
Case III	29%-intensity, scaled $\pi^d = 0.3$ $/kW
Case IV	29%-intensity, scaled $\pi^d = 0.5$ $/kW

Table IV reported the average performance of BMPC and the benchmarks under forecast errors $\delta_r = \delta_a = \delta_e = \delta_m = 0.1$, where the reward and demand charge gap were both compared. BMPC consistently obtained the largest reward over all the cases (between 2.09% and 5.07% reward gap), and it always captured the optimal demand charge even though starting from a smaller value. When the traffic was less intense with a low demand charge price, *i.e.*, Case I, MPC-scaled was the second best method with 4.70% reward gap, whereas its demand charge was identical to MPC-w/o and LLF-LD. This indicates that such method had more revenue from charging

TABLE IV
AVERAGE PERFORMANCE OF BMPC AND BENCHMARKS UNDER 10% FORECAST ERRORS ($\delta_r = \delta_a = \delta_e = \delta_m = 0.1$)

Scheduling Method	BMPC		EMPC [32]		MPC-scaled		MPC-w/o		LLF-LD [27]	
Performance Measure[1](%)	RG	DCG	RG	DCG	RG	DCG	RG	DCG	RG	DCG
Case I	2.09	0.00	5.06	23.17	4.70	50.00	6.51	50.00	5.33	50.00
Case II	3.29	0.00	6.69	23.20	13.80	50.00	17.29	50.00	15.12	50.00
Case III	2.98	0.00	8.97	21.60	5.10	12.50	7.11	37.50	4.25	37.50
Case IV	5.07	0.00	12.51	21.66	13.34	12.50	18.02	37.50	13.02	37.50

TABLE V
AVERAGE PERFORMANCE OF BMPC AND BENCHMARKS UNDER 20% FORECAST ERRORS ($\delta_r = \delta_a = \delta_e = \delta_m = 0.2$)

Scheduling method	BMPC		EMPC [32]		MPC-scaled		MPC-w/o		LLF-LD [27]	
Performance measure[1](%)	RG	DCG	RG	DCG	RG	DCG	RG	DCG	RG	DCG
Case I	4.97	25.00	10.35	42.03	5.05	50.00	8.33	50.00	5.33	50.00
Case II	8.98	25.00	11.47	42.67	15.07	50.00	21.17	50.00	15.12	50.00
Case III	5.58	7.69	12.56	31.17	8.56	12.50	11.95	37.50	4.25	37.50
Case IV	10.52	7.69	19.07	33.62	17.03	12.50	23.17	37.50	13.02	37.50

[1] RG: reward gap to upper bound; DCG: demand charge gap to the optimal demand charge
[2] The average computation time of the BMPC problems for Case I, Case II, Case III and Case IV is 0.85s, 0.92s, 0.96s and 0.87s, respectively.

the EVs. However, LLF-LD outperformed MPC-scaled by around 1% when more demands were involved (see Case III) since more EVs would be reported inaccurately. When the demand charge price was high, *i.e.*, Case II and Case IV, EMPC [32] was the second best method (6.69% and 12.51% reward gap respectively) with around 22% demand charge gap. It was found that the reward from EMPC [32] was more sensitive to the intensity levels rather than demand charge prices, which might result from the predictions over the entire trajectories (see Appendix C). It was also worth noting that the demand charge was the major factor to determine the performance of MPC-w/o and LLF-LD, where MPC-w/o showed the least performance in each case and could reach over 18% reward gap.

Table V reported the performance of all the methods when all the forecast errors increased to 0.2. Generally, the reward gaps from MPC-based methods became larger than the previous case, while LLF-LD was not affected since its performance did not depend on any predictions. BMPC continued to be the best method in all the cases except 1.33% more reward gap than LLF-LD in Case III. This would result from the fact that BMPC took a block of controls based on the inaccurate information for the near future. To be more specific, BMPC committed to the charging actions $\{\mathbf{u}_t^*, \mathbf{u}_{t+1}^*, \cdots, \mathbf{u}_{t+\ell-1}^*\}$ after solving (10) at t. The subsequent actions from $\mathbf{u}_t^*$, which were optimal for the predicted EV trajectory, would become sub-optimal for the realized EV profile. Such impact to lose the schedule revenue would become more dominant when the forecast error was larger under heavier traffics. On the other hand, although BMPC did not follow the optimal demand charge when ϕ_0 was 20% less than the optimal peak, it produced the closest gap between 7.69% and 25.00% among all the benchmarks.

Similarly to Table IV, MPC-scaled had good performance with just 0.08% and 3.02% less reward than BMPC in Case I and Case III, respectively, and thus showed that the fix weight W/T on the demand charge was only able to handle low demand charge prices. EMPC [32], however, was dramatically affected by the increase of the forecast error in both reward and demand charge, causing nearly 20% reward gap in Case IV. Although MPC-w/o still produced the same demand charge as LLF-LD, their reward gap was getting larger to over 10% since more forecast errors were imposed to the forecast window.

V. CONCLUSION

We consider the problem of EV-DC to maximize the reward from charging services at a charging station. Due to the difficulties of multiple timescales posed by the demand charge pricing, we propose the BMPC algorithm with a special end-of-horizon cost to incorporate the demand charge at each stage optimization, and the optimality conditions of the proposed method are presented and analyzed based on characterized demand patterns. Through the simulations on the ACN testbed, our proposed approach shows advantageous performances compared to the benchmark methods, highlighting the significant impact of demand charge on the EV charging scheduling.

APPENDIX A
PROOF OF PROPOSITION 1

Proof: We first show that the original EV-DC problem (7) can be decomposed by t^d. For a given trajectory $\boldsymbol{\xi}$ and $\mathbf{x}_0$, We rewrite (7) in the deterministic form:

$$\max_{\{\mathbf{u}_t\}_{t\in\mathcal{T}}} \; J_{\boldsymbol{\xi}}(\mathbf{x}_0) = \sum_{t=0}^{T-1} \mathcal{G}(\mathbf{x}_t, \mathbf{u}_t, \boldsymbol{\xi}_t) - \mathcal{C}(\psi_{\boldsymbol{\xi}})$$
$$\text{s.t. } (1)(2)(3)(4) \tag{18}$$

We denote $\mathcal{T}^d = \{t_p^d, p = 1, \ldots, P\}$ as the set of the decoupling intervals over trajectory $\boldsymbol{\xi}$. For each t_p^d where $(\mathbf{x}_{t_p^d}, \boldsymbol{\xi}_{t_p^d}) = (0, 0)$, the system state at $t_p^d + 1$ is not relevant to the previous states, *i.e.*, (1) is decoupled. Since the energy

requests before t_p^d cannot be deferred to intervals after t_p^d+1, the EV-DC problem (7) can be decomposed into $P+1$ segments: $\mathcal{S}(0)=\{0,\dots,t_1^d-1\}$, $\mathcal{S}(p)=\{t_p^d,\dots,t_{p+1}^d-1\}$ $(1\le p<P)$, and $\mathcal{S}(P)=\{t_P^d,\dots,T-1\}$. Let the optimal reward of (7) be $J_{\boldsymbol{\xi}}^*(\mathbf{x}_0)$ and the optimal solution $\mathbf{u}^*$, then we have:

$$J_{\boldsymbol{\xi}}^*(\mathbf{x}_0)=J_{\boldsymbol{\xi},\mathcal{S}(0)}^*(\mathbf{x}_0)+\sum_{p=1}^{P-1}J_{\boldsymbol{\xi},\mathcal{S}(p)}^*(\mathbf{x}_{t_p^d})+J_{\boldsymbol{\xi},\mathcal{S}(P)}^*(\mathbf{x}_{t_P^d})-\mathcal{C}\left(\max\left(\psi_{\boldsymbol{\xi},\mathcal{S}(0)}^*,\max_{1\le p<P}\psi_{\boldsymbol{\xi},\mathcal{S}(p)}^*,\psi_{\boldsymbol{\xi},\mathcal{S}(P)}^*\right)\right),\tag{19}$$

where

$$J_{\boldsymbol{\xi},\mathcal{S}(0)}^*(\mathbf{x}_0)=\sum_{t=0}^{t_1^d-1}\mathcal{G}(\mathbf{x}_t,\mathbf{u}_t^*,\boldsymbol{\xi}_t),\tag{20a}$$

$$J_{\boldsymbol{\xi},\mathcal{S}(p)}^*(\mathbf{x}_{t_p^d})=\sum_{t=t_p^d}^{t_{p+1}^d-1}\mathcal{G}(\mathbf{x}_t,\mathbf{u}_t^*,\boldsymbol{\xi}_t),\ \ 1\le p<P,\tag{20b}$$

$$J_{\boldsymbol{\xi},\mathcal{S}(P)}^*(\mathbf{x}_{t_P})=\sum_{t=t_P}^{T-1}\mathcal{G}(\mathbf{x}_t,\mathbf{u}_t^*,\boldsymbol{\xi}_t),\tag{20c}$$

$$\psi_{\boldsymbol{\xi},\mathcal{S}(0)}^*=\max_{t\in\mathcal{S}(0)}\sum_{i=1}^{N}u_{i,t}^*,\tag{20d}$$

$$\psi_{\boldsymbol{\xi},\mathcal{S}(p)}^*=\max_{t\in\mathcal{S}(p)}\sum_{i=1}^{N}u_{i,t}^*,\ \ 1\le p<P,\tag{20e}$$

$$\psi_{\boldsymbol{\xi},\mathcal{S}(P)}^*=\max_{t\in\mathcal{S}(P)}\sum_{i=1}^{N}u_{i,t}^*.\tag{20f}$$

where (20d), (20e) and (20f) are the results based on Assumption 1. Let $\psi_{\boldsymbol{\xi}}^*$ be the optimal maximum consumption of (7), which is clearly the maximum of (20d), (20e) and (20f). We also denote X^* and U^* as the optimal system state and solution set of the problem (7), respectively.

Then we show that for each segment above, the corresponding BMPC (10) reaches an optimal solution. Suppose BMPC operates at $t=0$. The first optimality condition is equivalent to $W\ge\max(t_1^d,\max_{k=1,\dots,P-1}(t_{k+1}-t_k),T-t_P^d)$, *i.e.*, the length of the forecast window is no shorter than the largest gap of adjacent decoupling intervals. Thus, the current BMPC can be decomposed into two sub-problems by t_1^d, as shown below[10]

$\mathcal{SP}(\text{BMPC})-\mathcal{S}(0)$:

$$\max_{\mathbf{u}'\in\mathcal{S}(0)}J_{\boldsymbol{\xi},\mathcal{S}(0)}(\mathbf{x}_0',\phi_0)=\sum_{k=0}^{t_1^d-1}\mathcal{G}(\mathbf{x}_k',\mathbf{u}_k',\hat{\boldsymbol{\xi}}_k)-\mathcal{C}(\phi_{t_1^d}-\phi_0)\tag{21a}$$

$$\text{s.t. }(10b)(10c)(10d)(10e)\tag{21b}$$

$$\mathbf{x}_0'=\mathbf{x}_0,\tag{21c}$$

[10]Here to distinguish from (7), we use $\mathbf{x}'$ and $\mathbf{u}'$ to represent the system state and the decision variable used in all the BMPC problems, respectively.

$\mathcal{SP}(\text{BMPC})-\mathcal{S}'(0)=\{t_1^d,\dots,W-1\}$:

$$\max_{\mathbf{u}'\in\mathcal{S}'(0)}J_{\boldsymbol{\xi},\mathcal{S}'(0)}(\mathbf{x}'_{t_1^d},\phi_{t_1^d})=\sum_{k=t_1^d}^{W-1}\mathcal{G}(\mathbf{x}_k',\mathbf{u}_k',\hat{\boldsymbol{\xi}}_k)-\mathcal{C}(\phi_{t+W}-\phi_{t_1^d})\tag{22a}$$

$$\text{s.t. }(10b)(10c)(10d)(10e)\tag{22b}$$

According to A8, $\{\hat{\boldsymbol{\xi}}_k\}_{k=0}^{t_1^d}=\{\boldsymbol{\xi}_t\}_{t=0}^{t_1^d}$, *i.e.*, the scheduler knows the accurate information to solve (21). The second optimality condition shows that $\phi_0=\psi_{\boldsymbol{\xi}}^*$, which indicates that $\phi_0\ge\psi_{\boldsymbol{\xi},\mathcal{S}(0)}^*$. Without loss of generality, two cases are discussed.

1) $\psi_{\boldsymbol{\xi}}^*$ Happens in $\mathcal{S}(0)$: We have $\phi_{t_1^d}^*=\phi_0=\psi_{\boldsymbol{\xi}}^*=\psi_{\boldsymbol{\xi},\mathcal{S}(0)}^*$ since the scheduler would not necessarily rise the consumption level beyond the optimal one. Otherwise, more penalty from demand charge would reduce the total reward of the segment $\mathcal{S}(0)$. In other words, the optimal reward of (21) is the identical to $J_{\boldsymbol{\xi},\mathcal{S}(0)}^*(\mathbf{x}_0)$.

2) $\psi_{\boldsymbol{\xi}}^*$ Happens Out of $\mathcal{S}(0)$: It is obvious that $\phi_0>\psi_{\boldsymbol{\xi},\mathcal{S}(0)}^*$. This provides a higher threshold on the maximum consumption of the segment $\mathcal{S}(0)$, and indicates that the last term of (21a) is not effective. Hence, the scheduler would not take demand charge into consideration so that the optimal reward of (21) is also identical to the $J_{\boldsymbol{\xi},\mathcal{S}(0)}^*(\mathbf{x}_0)$, where the latter also ignores the demand charge in the one-shot solution.

Consequently, for both cases shown above, we have the optimal reward of (21) $J_{\boldsymbol{\xi},\mathcal{S}(0)}^*(\mathbf{x}_0',\phi_0)=J_{\boldsymbol{\xi},\mathcal{S}(0)}^*(\mathbf{x}_0)$, and the optimal solution $\mathbf{u}_0'^*$ of (21) must be within the optimal set U^*, *i.e.*, $\mathbf{u}_0'^*\in U^*$.

Then the system updates to $\mathbf{x}_1'$ and we have $\mathbf{x}_1'\in X^*$ and $\phi_1=\phi_0=\psi_{\boldsymbol{\xi}}^*$. Then we assume $t_1^d>1$ (this would not make any difference if $t_1^d=1$). Similarly to the above, the new forecast window still contains t_1^d so that the new BMPC problem can also be decomposed into two sub-problems as follows:

$\mathcal{SP}(\text{BMPC})-\mathcal{S}(0,0)=\mathcal{S}(0)\setminus\{0\}$:

$$\max_{\mathbf{u}'\in\mathcal{S}(0,0)}J_{\boldsymbol{\xi},\mathcal{S}(0,0)}(\mathbf{x}'_1,\phi_1)=\sum_{k=1}^{t_1^d-1}\mathcal{G}(\mathbf{x}_k',\mathbf{u}_k',\hat{\boldsymbol{\xi}}_k)-\mathcal{C}(\phi_{t_1^d}-\phi_1)\tag{23a}$$

$$\text{s.t. }(10b)(10c)(10d)(10e)\tag{23b}$$

$\mathcal{SP}(\text{BMPC})-\mathcal{S}'(0)$: see (22)

The last term of (23a) follows the same rule as discussed above. Based on the Principle of Optimality, we have $J_{\boldsymbol{\xi},\mathcal{S}(0)}^*(\mathbf{x}_1',\phi_1)$ the optimal reward from $t=1$ to t_1^d-1 and thus $\mathbf{u}_1'^*\in U^*$. As BMPC rolls to the subsequent stage starting at t_1^d-1, BMPC always produces the optimal solutions, thus we have

$$\sum_{t=0}^{t_1^d-1}\mathcal{G}(\mathbf{x}_t',\mathbf{u}_t'^*,\boldsymbol{\xi}_t)=J_{\boldsymbol{\xi},\mathcal{S}(0)}^*(\mathbf{x}_0),\tag{24}$$

where the left hand side is the total reward produced by BMPC from $t=1$ to t_1^d-1. And then BMPC starts at $t=t_1^d$ and repeats as above until the last segment $\mathcal{S}(P)$. Consequently,

we have

$$\sum_{t=t_p^d}^{t_{p+1}^d-1} \mathcal{G}(\mathbf{x}'_t, \mathbf{u}'^*_t, \boldsymbol{\xi}_t) = J^*_{\boldsymbol{\xi},\mathcal{S}(p)}(\mathbf{x}_{t_p^d}), \ \forall 1 \le p < P, \tag{25}$$

$$\sum_{t=t_P^d}^{T-1} \mathcal{G}(\mathbf{x}'_t, \mathbf{u}'^*_t, \boldsymbol{\xi}_t) = J^*_{\boldsymbol{\xi},\mathcal{S}(P)}(\mathbf{x}_{t_P^d}). \tag{26}$$

and

$$\phi_T = \phi_{T-1} = \cdots = \phi_0 = \psi^*_{\boldsymbol{\xi}}. \tag{27}$$

According to (19)(20) and (24)-(27), we have

$$J^{\text{BMPC}}_{\boldsymbol{\xi}}(\mathbf{x}'_0, \phi_0) = \sum_{t=0}^{T-1} \mathcal{G}(\mathbf{x}'_t, \mathbf{u}'^*_t, \boldsymbol{\xi}_t) - \mathcal{C}(\phi_T) = J^*_{\boldsymbol{\xi}}(\mathbf{x}_0), \tag{28}$$

and thus BMPC produces an optimal solution. □

APPENDIX B
BENCHMARKS

1) MPC With Scaled Demand Charge (MPC-Scaled): MPC-scaled imposes a fraction of the demand charge in each rolling-window optimization, and such form is adopted in [31]. At each $t \in \mathcal{T}$, MPC-scaled solves the following problem:

$$\begin{aligned}\max_{\{\mathbf{u}_k\}_{t\in\mathcal{T}}} \ J_t^{\text{MPC-scaled}} := & \sum_{k=t}^{t+W-1} \mathcal{G}(\mathbf{x}_k, \mathbf{u}_k, \hat{\boldsymbol{\xi}}_k) \\ & - \frac{W}{T}\mathcal{C}\left(\max_{k\in[t,t+W-1]}\left(\sum_{i=1}^{N} u_{i,k}\right)\right) \\ \text{s.t. } & (10b)(10c)(10d).\end{aligned} \tag{29}$$

Unlike BMPC, only the optimal control $\mathbf{u}_t^*$ will be implemented and the temporal structure of MPC-scaled is identical to the nominal MPC.

2) EMPC [32]: EMPC [32] aims to track a predetermined reference schedule with the consideration of demand charge for the setting that $\ell = 1$. Here we present a slight modification of EMPC [32] so that it applies to cases when $\ell > 1$.

Let $(\mathbf{x}^{\text{ref}}, \mathbf{u}^{\text{ref}}, \boldsymbol{\xi}^{\text{ref}})$ be an arbitrarily known reference trajectory over $\mathcal{T}$ (see Appendix C for the reference trajectory). For each $t \in \mathcal{T}$, the objective of EMPC [32] is defined as

$$\begin{aligned}J_t^{\text{EMPC}} := & \sum_{k=t}^{t+W-1} \mathcal{G}_k(\mathbf{x}_k, \mathbf{u}_k, \boldsymbol{\xi}_k^{\text{ref}}) \\ & - \mathcal{C}(\max(\phi_{t+W}, \breve{\psi}_{t+W}^{\text{ref}})) - \mathcal{C}(\psi^{\text{ref}}),\end{aligned} \tag{30}$$

where parameters ψ^{ref} and $\breve{\psi}_{t+W}^{\text{ref}}$ denote the peak consumption over the entire (from 0 to $T-1$) and the remaining horizon (from $t+W$ to $T-1$) of the reference trajectory respectively, and are computed as

$$\psi^{\text{ref}} := \max_{t\in\mathcal{T}'} \left\{\frac{1}{\ell}\sum_{\tau=t}^{t+\ell}\sum_{i=1}^{N} u_{i,\tau}^{\text{ref}}\right\}, \tag{31}$$

$$\breve{\psi}_t^{\text{ref}} := \max_{k\in\mathcal{T}', k\ge t} \left\{\frac{1}{\ell}\sum_{\tau=k}^{k+\ell-1}\sum_{i=1}^{N} u_{i,\tau}^{\text{ref}}\right\}, \ t \in \mathcal{T}. \tag{32}$$

At $t \in \mathcal{T}$ with the system state $\mathbf{x}_t$ and ϕ_t, EMPC can be formulated as

$$\max_{\{\mathbf{u}_k\}_{k=t}^{t+W-1}} \ J_t^{\text{EMPC}}$$

$$\text{s.t. } x_{i,k+1} = \begin{cases} x_{i,k} - (u_{i,k}, 1) & \text{if } \tau_{i,k} > 1, \\ \xi_{i,k}^{\text{ref}} & \text{if } \tau_{i,k} \le 1. \end{cases}, \tag{33a}$$

$$\sum_{i=1}^{N} u_{i,k} \le M, \tag{33b}$$

$$u_{i,k} \le x_{i,k}, \ i \in \{1, \ldots, N\} \tag{33c}$$

$$\phi_{k+1} = \max(\phi_k, \sum_{i=1}^{N} u_{i,k}) \tag{33d}$$

$$k = t, \ldots, t+W-1,$$

$$\mathbf{x}_{t+W} = \mathbf{x}_{t+W}^{\text{ref}}, \tag{33e}$$

Note that the temporal structure is also the same as the nominal MPC.

3) MPC Without Demand Charge (MPC-w/O): MPC-w/o follows the framework of the nominal MPC, that moves only one interval at each time, *i.e.*, solving the following optimization problem consisting of W intervals at every $t \in \mathcal{T}$ starting at current state $\mathbf{x}_t$:

$$\begin{aligned}\max \ J_t^{\text{MPC-w/o}} := & \sum_{k=t}^{t+W-1} \mathcal{G}(\mathbf{x}_k, \mathbf{u}_k, \hat{\xi}_k) \\ \text{s.t. } & (10b)(10c)(10d).\end{aligned} \tag{34}$$

Note that MPC-w/o does not take demand charge into consideration, which is another major difference from BMPC.

4) LLF-LD [27]: LLF-LD is an online algorithm for deferrable load scheduling, which prioritizes tasks with less laxity at each interval. Laxity, as defined in [27], is the difference between a server's lead time and its remaining processing time, reflecting the maximum number of intervals that a task can tolerate before the time it has to be continuously processed to avoid non-completion penalty. For the EV-DC problem in Section II, the laxity of an EV at charger i at t is $\tau_{i,t} - r_{i,t}$. If the laxity of two tasks are the same, then it prioritizes the one with later deadline. Note that the available total charging power at each interval for LLF-LD is always MR. Based on the LLF-LD rule, the scheduler assigns each unit of charging power to each unfinished EVs from the top priority to the bottom (or until all the MR charging power has been scheduled). If the number of unfinished EVs is greater than M, then the scheduler would leave the rest to the next interval. Thus, LLF-LD could yield significant demand charge when the traffic is intensive.

APPENDIX C
REFERENCE TRAJECTORY OF EMPC [32]

The reference trajectory sets the states and decisions for the EMPC to track. Here we consider to generate the reference trajectory by solving the EV-DC problem (7) in one-shot, and therefore the whole trajectory of all the EVs must be forecast,

i.e., from $t = 0$ to $T - 1$. We denote $\{\boldsymbol{\xi}_t^{\text{ref}}\}_{t\in\mathcal{T}}$ as the forecast EV loads, then the reference trajectory can be computed by the following deterministic EV-DC problem:

$$\begin{aligned} \max_{\{\mathbf{u}_t\}_{t\in\mathcal{T}}} \quad & \sum_{t\in\mathcal{T}} \mathcal{G}_t(\mathbf{x}_t, \mathbf{u}_t, \boldsymbol{\xi}_t^{\text{ref}}) - \mathcal{C}(\psi) \\ \text{s.t. } x_{i,t+1} = & \begin{cases} x_{i,t} - (u_{i,t}, 1) & \text{if } \tau_{i,t} > 1, \\ \xi_{i,t}^{\text{ref}} & \text{if } \tau_{i,t} \le 1, \end{cases} \\ & \text{and } (2)(3)(4), \end{aligned} \tag{35}$$

By denoting $(\mathbf{x}^{\text{ref}}, \mathbf{u}^{\text{ref}})$ as the optimal solution of (35), the reference trajectory can be obtained as $(\mathbf{x}^{\text{ref}}, \mathbf{u}^{\text{ref}}, \boldsymbol{\xi}^{\text{ref}})$.

REFERENCES

[1] K. Clement-Nyns, E. Haesen, and J. Driesen, "The impact of charging plug-in hybrid electric vehicles on a residential distribution grid," *IEEE Trans. Power Syst.*, vol. 25, no. 1, pp. 371–380, Feb. 2009.

[2] Z. Ma, D. S. Callaway, and I. A. Hiskens, "Decentralized charging control of large populations of plug-in electric vehicles," *IEEE Trans. Control Syst. Technol.*, vol. 21, no. 1, pp. 67–78, Dec. 2012.

[3] L. Gan, U. Topcu, and S. H. Low, "Optimal decentralized protocol for electric vehicle charging," *IEEE Trans. Power Syst.*, vol. 28, no. 2, pp. 940–951, May 2013.

[4] J. Rivera, C. Goebel, and H.-A. Jacobsen, "Distributed convex optimization for electric vehicle aggregators," *IEEE Trans. Smart Grid*, vol. 8, no. 4, pp. 1852–1863, Jul. 2017.

[5] C. Le Floch, S. Bansal, C. J. Tomlin, S. J. Moura, and M. N. Zeilinger, "Plug-and-play model predictive control for load shaping and voltage control in smart grids," *IEEE Trans. Smart Grid*, vol. 10, no. 3, pp. 2334–2344, May 2019.

[6] Y. Yang, Q.-S. Jia, X. Guan, X. Zhang, Z. Qiu, and G. Deconinck, "Decentralized EV-based charging optimization with building integrated wind energy," *IEEE Trans. Autom. Sci. Eng.*, vol. 16, no. 3, pp. 1002–1017, Jul. 2019.

[7] K. Ojand and H. Dagdougui, "Q-learning-based model predictive control for energy management in residential aggregator," *IEEE Trans. Autom. Sci. Eng.*, vol. 19, no. 1, pp. 70–81, Jan. 2022.

[8] Z. J. Lee et al., "Adaptive charging networks: A framework for smart electric vehicle charging," *IEEE Trans. Smart Grid*, vol. 12, no. 5, pp. 4339–4350, Sep. 2021.

[9] Z. J. Lee, S. Sharma, D. Johansson, and S. H. Low, "ACN-Sim: An open-source simulator for data-driven electric vehicle charging research," *IEEE Trans. Smart Grid*, vol. 12, no. 6, pp. 5113–5123, Nov. 2021.

[10] C. L. Liu and J. W. Layland, "Scheduling algorithms for multiprogramming in a hard-real-time environment," *J. ACM*, vol. 20, no. 1, pp. 46–61, 1973.

[11] A. K.-L. Mok, "Fundamental design problems of distributed systems for the hard-real-time environment," Ph.D. dissertation, Massachusetts Inst. Technol., Cambridge, MA, USA, 1983.

[12] S. S. Panwar, D. Towsley, and J. K. Wolf, "Optimal scheduling policies for a class of queues with customer deadlines to the beginning of service," *J. ACM*, vol. 35, no. 4, pp. 832–844, 1988.

[13] S. Chen, L. Tong, and T. He, "Optimal deadline scheduling with commitment," in *Proc. 49th Annu. Allerton Conf. Commun., Control, Comput. (Allerton)*, Sep. 2011, pp. 111–118.

[14] A. Subramanian, M. J. Garcia, D. S. Callaway, K. Poolla, and P. Varaiya, "Real-time scheduling of distributed resources," *IEEE Trans. Smart Grid*, vol. 4, no. 4, pp. 2122–2130, Dec. 2013.

[15] N. Chen, C. Kurniawan, Y. Nakahira, L. Chen, and S. H. Low, "Smoothed least-laxity-first algorithm for electric vehicle charging: Online decision and performance analysis with resource augmentation," *IEEE Trans. Smart Grid*, vol. 13, no. 3, pp. 2209–2217, May 2022.

[16] Y. Xu and F. Pan, "Scheduling for charging plug-in hybrid electric vehicles," in *Proc. IEEE 51st IEEE Conf. Decis. Control (CDC)*, Dec. 2012, pp. 2495–2501.

[17] Z. Yu, Y. Xu, and L. Tong, "Large scale charging of electric vehicles: A multi-armed bandit approach," in *Proc. 53rd Annu. Allerton Conf. Commun., Control, Comput. (Allerton)*, Sep. 2015, pp. 389–395.

[18] Q. Huang, Q. S. Jia, Z. Qiu, X. Guan, and G. Deconinck, "Matching EV charging load with uncertain wind: A simulation-based policy improvement approach," *IEEE Trans. Smart Grid*, vol. 6, no. 3, pp. 1425–1433, May 2015.

[19] Q. Huang, Q.-S. Jia, and X. Guan, "A multi-timescale and bilevel coordination approach for matching uncertain wind supply with EV charging demand," *IEEE Trans. Autom. Sci. Eng.*, vol. 14, no. 2, pp. 694–704, Apr. 2016.

[20] Z. Jiang, Q. Jia, and X. Guan, "A computing budget allocation method for minimizing EV charging cost using uncertain wind power," *IEEE Trans. Autom. Sci. Eng.*, vol. 18, no. 2, pp. 681–692, Apr. 2021.

[21] Y. Xu, F. Pan, and L. Tong, "Dynamic scheduling for charging electric vehicles: A priority rule," *IEEE Trans. Autom. Control*, vol. 61, no. 12, pp. 4094–4099, Dec. 2016.

[22] J. Jin and Y. Xu, "Joint scheduling of electric vehicle charging and energy storage operation," in *Proc. IEEE Conf. Decis. Control (CDC)*, Dec. 2018, pp. 4103–4109.

[23] Z. Yu, Y. Xu, and L. Tong, "Deadline scheduling as restless bandits," *IEEE Trans. Autom. Control*, vol. 63, no. 8, pp. 2343–2358, Aug. 2018.

[24] L. Hao and Y. Xu, "Index policies for stochastic deadline scheduling with time-varying processing rate limits," in *Proc. Amer. Control Conf. (ACC)*, Jul. 2020, pp. 204–210.

[25] J. Jin and Y. Xu, "Optimal policy characterization enhanced actor-critic approach for electric vehicle charging scheduling in a power distribution network," *IEEE Trans. Smart Grid*, vol. 12, no. 2, pp. 1416–1428, Mar. 2021.

[26] P. Whittle, "Restless bandits: Activity allocation in a changing world," *J. Appl. Probab.*, vol. 25, pp. 287–298, Jan. 1988.

[27] J. Jin, L. Hao, Y. Xu, J. Wu, and Q.-S. Jia, "Joint scheduling of deferrable demand and storage with random supply and processing rate limits," *IEEE Trans. Autom. Control*, vol. 66, no. 11, pp. 5506–5513, Nov. 2021.

[28] M. Ellis, H. Durand, and P. D. Christofides, "A tutorial review of economic model predictive control methods," *J. Process Control*, vol. 24, no. 8, pp. 1156–1178, Aug. 2014.

[29] R. Halvgaard, N. K. Poulsen, H. Madsen, J. B. Jorgensen, F. Marra, and D. E. M. Bondy, "Electric vehicle charge planning using economic model predictive control," in *Proc. IEEE Int. Electr. Vehicle Conf.*, Mar. 2012, pp. 1–6.

[30] J. Engel, T. Schmitt, T. Rodemann, and J. Adamy, "Hierarchical economic model predictive control approach for a building energy management system with scenario-driven EV charging," *IEEE Trans. Smart Grid*, vol. 13, no. 4, pp. 3082–3093, Jul. 2022.

[31] R. Kumar, M. J. Wenzel, M. J. Ellis, M. N. ElBsat, K. H. Drees, and V. M. Zavala, "A stochastic model predictive control framework for stationary battery systems," *IEEE Trans. Power Syst.*, vol. 33, no. 4, pp. 4397–4406, Jul. 2018.

[32] M. J. Risbeck and J. B. Rawlings, "Economic model predictive control for time-varying cost and peak demand charge optimization," *IEEE Trans. Autom. Control*, vol. 65, no. 7, pp. 2957–2968, Jul. 2020.

[33] M. Dabbagh, B. Hamdaoui, A. Rayes, and M. Guizani, "Shaving data center power demand peaks through energy storage and workload shifting control," *IEEE Trans. Cloud Comput.*, vol. 7, no. 4, pp. 1095–1108, Oct. 2019.

[34] J. Jin and Y. Xu, "Optimal storage operation under demand charge," *IEEE Trans. Power Syst.*, vol. 32, no. 1, pp. 795–808, Jan. 2017.

[35] S. Chen and L. Tong, "IEMS for large scale charging of electric vehicles: Architecture and optimal online scheduling," in *Proc. IEEE 3rd Int. Conf. Smart Grid Commun. (SmartGridComm)*, Nov. 2012, pp. 629–634.

[36] Z. Yu, S. Chen, and L. Tong, "An intelligent energy management system for large-scale charging of electric vehicles," *CSEE J. Power Energy Syst.*, vol. 2, no. 1, pp. 47–53, Mar. 2016.

[37] Y. Qin, Z. Bei, and M. Kezunovic, "Optimized operational cost reduction for an EV charging station integrated with battery energy storage and PV generation," *IEEE Trans. Smart Grid*, vol. 10, no. 2, pp. 2096–2106, Mar. 2018.

[38] M. S. Athulya, A. Visakh, and M. P. Selvan, "Electric vehicle recharge scheduling in a shopping mall charging station," in *Proc. 21st Nat. Power Syst. Conf. (NPSC)*, Dec. 2020, pp. 1–6.

[39] H. Zhang, Z. Hu, Z. Xu, and Y. Song, "Optimal planning of PEV charging station with single output multiple cables charging spots," *IEEE Trans. Smart Grid*, vol. 8, no. 5, pp. 2119–2128, Sep. 2017.

[40] M. Yilmaz and P. T. Krein, "Review of battery charger topologies, charging power levels, and infrastructure for plug-in electric and hybrid vehicles," *IEEE Trans. Power Electron.*, vol. 28, no. 5, pp. 2151–2169, May 2013.
[41] L. Zhang, M. Yang, and Z. Zhao, "Game analysis of charging service fee based on benefit of multi-party participants: A case study analysis in China," *Sustain. Cities Soc.*, vol. 48, Jan. 2019, Art. no. 101528.
[42] E. Bitar and Y. Xu, "Deadline differentiated pricing of deferrable electric loads," *IEEE Trans. Smart Grid*, vol. 8, no. 1, pp. 13–25, Jan. 2017.
[43] Y. Kim, J. Kwak, and S. Chong, "Dynamic pricing, scheduling, and energy management for profit maximization in PHEV charging stations," *IEEE Trans. Veh. Technol.*, vol. 66, no. 2, pp. 1011–1026, Feb. 2017.
[44] H. Chen, Z. Hu, H. Luo, J. Qin, R. Rajagopal, and H. Zhang, "Design and planning of a multiple-charger multiple-port charging system for PEV charging station," *IEEE Trans. Smart Grid*, vol. 10, no. 1, pp. 173–183, Jan. 2017.
[45] N. Machiels, N. Leemput, F. Geth, J. Van Roy, J. Büscher, and J. Driesen, "Design criteria for electric vehicle fast charge infrastructure based on flemish mobility behavior," *IEEE Trans. Smart Grid*, vol. 5, no. 1, pp. 320–327, Jan. 2014.
[46] M. Rahmani-Andebili, "Scheduling deferrable appliances and energy resources of a smart home applying multi-time scale stochastic model predictive control," *Sustain. Cities Soc.*, vol. 32, pp. 338–347, Jul. 2017.
[47] Gurobi. *Gurobi 9.5 Performance Benchmarks*. Accessed: Nov. 1, 2022. [Online]. Available: https://www.gurobi.com/features/gurobi-optimizer-delivers-unmatched-performance
[48] *CPLEX Optimization Studio 12.10 Performance Improvements*. Accessed: Nov. 1, 2022. [Online]. Available: https://www.ibm.com/products/ilog-cplex-optimization-studio/cplex-optimizer
[49] W. Charytoniuk, M. S. Chen, P. Kotas, and P. V. Olinda, "Demand forecasting in power distribution systems using nonparametric probability density estimation," *IEEE Trans. Power Syst.*, vol. 14, no. 4, pp. 1200–1206, Nov. 1999.
[50] A. K. Singh, S. Khatoon, M. Muazzam, and D. K. Chaturvedi, "Load forecasting techniques and methodologies: A review," in *Proc. 2nd Int. Conf. Power, Control Embedded Syst.*, Dec. 2012, pp. 1–10.
[51] V. Jain, A. Sharma, and L. Subramanian, "Road traffic congestion in the developing world," in *Proc. 2nd ACM Symp. Comput. Develop.*, Mar. 2012, pp. 1–10.
[52] Z. J. Lee, T. Li, and S. H. Low, "ACN-Data: Analysis and applications of an open EV charging dataset," in *Proc. 10th ACM Int. Conf. Future Energy Syst.*, Jun. 2019, pp. 139–149.

Lei Yang (Student Member, IEEE) received the B.E. degree from Zhejiang University, Hangzhou, China, in 2014, and the M.Sc. degree from the University of Bristol, Bristol, U.K., in 2016. He is currently pursuing the Ph.D. degree with the Department of Electronic and Information Engineering, Xi'an Jiaotong University, Xi'an, China.

He was a Visiting Student with Cornell University, Ithaca, NY, USA, in 2020. His current research interests include energy and power systems, smart city, and the integration of transportation and information systems. His expertise lies in Markov decision process, optimization, and model predictive control.

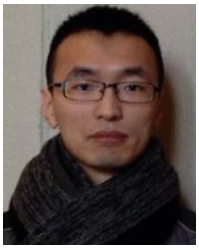

Xinbo Geng (Member, IEEE) received the B.E. degree in electrical engineering from Tsinghua University, Beijing, China, in 2013, and the M.S. and Ph.D. degrees in electrical engineering from the Department of Electrical and Computer Engineering, Texas A&M University, College Station, TX, USA, in 2015 and 2019, respectively.

He was a Power System Design and Studies Intern with the National Renewable Energy Laboratory in 2016; a Data Analyst Intern with ISO New England in 2017; a Visiting Student with the University of California at Berkeley and the Massachusetts Institute of Technology, Cambridge, MA, USA, in 2018; a Visiting Student with the University of Wisconsin–Madison, Madison, WI, USA, in 2019; and a Post-Doctoral Researcher jointly affiliated with Cornell University, Ithaca, NY, USA, and Texas A&M University from 2020 to 2021. His research interests include decision-making under uncertainties.

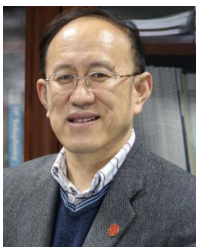

Xiaohong Guan (Life Fellow, IEEE) received the B.S. and M.S. degrees in control engineering from Tsinghua University, Beijing, China, in 1982 and 1985, respectively, and the Ph.D. degree in electrical and systems engineering from the University of Connecticut, Storrs, in 1993.

He was a Senior Consulting Engineer with Pacific Gas and Electric from 1993 to 1995. He visited the Division of Engineering and Applied Science, Harvard University, from 1999 to 2000. From 1985 to 1988 and since 1995, he has been with Xi'an Jiaotong University, Xi'an, China. He has been the Cheung Kong Professor of Systems Engineering since 1999. He was the Director of the State Key Laboratory for Manufacturing Systems from 1999 to 2009 and the Dean of the School of Electronic and Information Engineering from 2008 to 2018. Since 2001, he has also been with the Center for Intelligent and Networked Systems, Tsinghua University, where was the Head of the Department of Automation from 2003 to 2008. He has been the Dean of the Faculty of Electronic and Information Engineering since 2019. His research interests include economics and security of networked systems, including power and energy systems, manufacturing systems, and cyber-physical systems. He is a member of the Chinese Academy of Sciences.

Lang Tong (Fellow, IEEE) received the B.E. degree from Tsinghua University, Beijing, China, in 1985, and the Ph.D. degree from the University of Notre Dame, USA, in 1991.

He was a Post-Doctoral Research Affiliate with Stanford University. He held visiting positions at Stanford University, the University of California at Berkeley, the Delft University of Technology, and the Chalmers University of Technology, Sweden. He is currently the Irwin and Joan Jacobs Professor of Engineering and the Cornell Site Director of the Power Systems Engineering Research Center (PSERC), Cornell University, Ithaca, NY, USA. His research interests include energy and power systems, electricity markets, smart grids, and the electrification of transportation systems. His expertise lies in data analytics, machine learning, optimization, and market design. He received numerous publication awards from the IEEE Signal Processing Society, the IEEE Communications Society, and the IEEE Power and Energy Systems Society. He was the 2018 Fulbright Distinguished Chair in Alternative Energy.